

# Fermions localized on solitons in flat and curved spacetime

**V Dzhunushaliev**

Department of Theoretical and Nuclear Physics, Al-Farabi Kazakh National University, Almaty 050040, Kazakhstan

**V Folomeev**

International Laboratory for Theoretical Cosmology, Tomsk State University of Control Systems and Radioelectronics (TUSUR), Tomsk 634050, Russia

**Ya Shnir**

Institute of Physics, Carl von Ossietzky University Oldenburg, Germany Oldenburg D-26111, Germany

**Abstract.** A brief overview of the fermionic modes localized on topological solitons is presented.

## 1 Introduction

One of the most interesting directions of research in theoretical physics over the past few decades has been the study of topological solitons, particle-like regular localized field configurations with finite energy. Topological solitons occur in various nonlinear classical field theories. Perhaps simplest examples are the kinks which appear in (1+1)-dimensional scalar models with a potential possessing two or more degenerated minima, see, e.g., Refs. [1, 2]. An interesting examples in (2+1) dimensions are Nielsen-Olesen vortices in the Abelian Higgs model [3] and soliton solutions of the non-linear  $O(3)$  sigma model [4]. Modification of the latter theory is known as the baby Skyrme model [5, 6] a planar reduction of the original Skyrme model in (3+1) dimensions [7]. Another famous example of topological solitons in (3+1) dimensions are monopoles in the Yang-Mills-Higgs model [8, 9].

Remarkable feature of the topological solitons is the relation between the topological charge of the configuration and the number of fermionic zero modes localized on a soliton. The fundamental Atiyah-Patodi-Singer index theorem requires one normalizable fermionic zero mode per unit topological charge [10]. Moreover, apart zero modes, most configurations also support existence of a tower of localized fermionic modes with non-zero energy.

The fermionic modes localized on solitons have been studied for many decades, starting from the pioneering paper [11], later revisited in [12], where fermion-vortex system was investigated. There has been much interest in studying the localized fermionic states in various systems; examples of such are fermion modes of the kinks [13, 14], monopoles [15, 16], and skyrmions [21, 22]. Existence of localized fermions leads to many intriguing and fascinating phenomena, such as fermion number fractionization [14, 12], Rubakov-Callan mechanism of monopole catalysis of proton decay [15, 16], and string superconductivity [17].



Notably, fermionic zero modes naturally appear in supersymmetric theories; several simple examples are  $N = 1$  chiral scalar superfield in (1+1) dimensions [18], supersymmetric extensions of the  $O(3)$  sigma model [19], and baby-Skyrme model [20]. In such situation the fermion zero modes are generated via SUSY transformations of the bosonic sector of a static soliton. The breaking of supersymmetry of the configurations, in agreement with the index theorem, shows a spectral flow of the eigenvalues of the Dirac operator with some number of normalizable bounded modes crossing zero.

The typical assumption in most of such considerations is that the spinor field does not backreact on the soliton [13, 14]; moreover, only the fermion zero modes were considered in most cases. This assumption is justified in the weak coupling limit. However, as the Yukawa coupling increases, the effects of the backreaction can be significant. A different approach to the problem was proposed recently in [23, 24, 25, 26] where backreaction of the localized fermions on solitons was taken into account. This concept was subsequently applied in modelling various dynamical systems [27, 28, 29, 30, 31].

The situation gets another twist as the gravitational interaction is taken into account. As compared to boson fields, fermions have attracted less consideration in General Relativity. Although solutions of the Dirac equation in curved spacetime were constructed many decades ago [32], the study of self-gravitating fermions still remains somewhat obscure, because the Dirac field has to be treated in terms of a normalizable quantum wave function. However, one can make use of certain restrictions supposing that only one-particle fermion modes are considered, and second quantization of the fields is ignored. In this framework gravitational interaction is treated purely classically. It then turns out that the system of the Einstein-Dirac equations supports regular localized solitonic solutions [33], the so-called Dirac stars [34, 35, 36, 37, 38]. Interestingly, the backreaction of self-gravitating fermions may significantly affect the metric and, in particular, allow for (traversable) wormholes [39, 40]. It was pointed out that self-gravitating spinor fields may give rise to some interesting phenomena in the cosmology of the accelerating Universe [41, 42]. Further, it was found recently that the localization of the backreacting fermionic mode on a Skyrminion may violate the energy conditions; as a result, regular self-gravitating asymptotically flat solutions with negative and zero ADM mass may emerge [43].

Below we briefly review recent works on solitons with localized backreacting fermions.

## 2 Fermion localization on the kinks

As a prototype model, which describes solitons with localized fermions in (1+1) dimensions, we consider the minimal  $N = 1$  supersymmetric sigma-model with the chiral scalar superfield  $\Phi(x, \theta) = \phi(x) + i\theta\psi(x) + \frac{i}{2}(\bar{\theta}\theta)F(x)$ , where  $\phi$  is a real scalar field,  $\psi$  is a fermion field and  $F$  is an auxiliary field [18]. In component notation the Lagrangian of the model is

$$L_{N=1} = \frac{1}{2} (\partial_\mu \phi)^2 + \frac{i}{2} \bar{\psi} \gamma^\mu \partial_\mu \psi + \frac{1}{2} F^2 + F W' - \frac{1}{2} W'' \bar{\psi} \psi, \quad (1)$$

where  $W$  is the so-called superpotential, the matrices  $\gamma_\mu$  are  $\gamma_0 = \sigma_1$ ,  $\gamma_1 = i\sigma_3$ , where  $\sigma_i$  are the Pauli matrices, and  $\bar{\psi} = \psi \gamma^0$ .

Since the Euler-Lagrange equation for the field  $F$  is just  $F = -W'$ , it can be eliminated, so the Lagrangian (1) becomes

$$L_{N=1} = \frac{1}{2} (\partial_\mu \phi)^2 + \frac{i}{2} \bar{\psi} \gamma^\mu \partial_\mu \psi - \frac{1}{2} W'' \bar{\psi} \psi - \frac{1}{2} (W')^2. \quad (2)$$

The supersymmetry transformations of the fields are

$$\delta \phi = \eta \psi, \quad \delta \psi = \eta (\gamma^\mu \partial_\mu \phi - W), \quad (3)$$

where  $\eta$  is a Grassmann valued parameter. A particular choice of the superpotential  $W' = \frac{1}{\sqrt{2}} (\phi^2 - 1)$  leads to the action of the  $\phi^4$  model with the double vacuum potential  $V = (W')^2$  coupled to the fermions via the fixed Yukawa coupling  $g = \sqrt{2}$ :

$$S = \frac{1}{2} \int d^2 x \left[ (\partial_\mu \phi)^2 + i \bar{\psi} \gamma^\mu \partial_\mu \psi - g \phi \bar{\psi} \psi - \frac{1}{2} (\phi^2 - 1)^2 \right]. \quad (4)$$

The supersymmetry of the model is violated as the Yukawa coupling becomes a free parameter, or as the potential  $V$  is no longer related to the prepotential  $W$ .

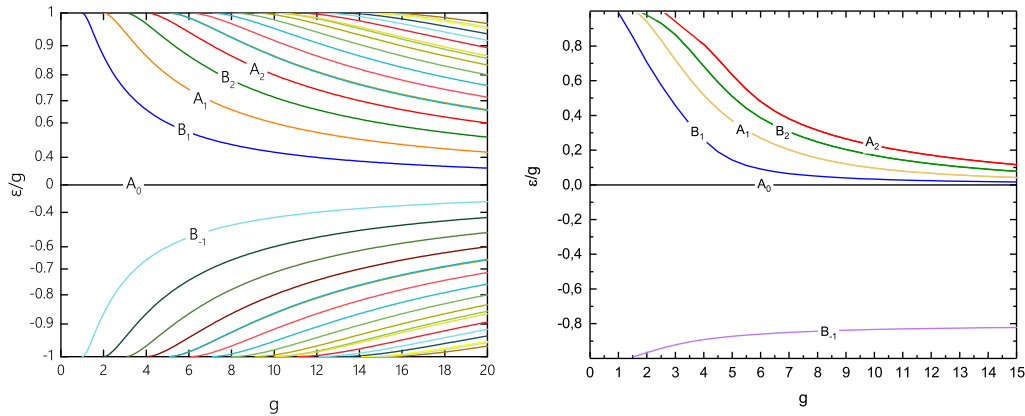


Figure 1: Normalized energy  $\frac{\epsilon}{g}$  of the localized fermionic states as a function of the Yukawa coupling  $g$  for several fermion modes at  $m = 0$  without backreaction (left panel) and with backreaction of the fermions on the kink (right panel). Reprinted (without modification) from Ref. [25], ©2019 The Authors of [25] under the CC BY 4.0 license.

The field equations of the model are given by

$$\begin{aligned} \partial_\mu \partial^\mu \phi + g \bar{\psi} \psi - \phi + \phi^3 &= 0, \\ i \gamma^\mu \partial_\mu \psi - g \phi \psi &= 0. \end{aligned} \quad (5)$$

Using the parametrization of the two-component spinor  $\psi^T = e^{-i\epsilon t}(u, v)$ , the equations (5) become:

$$\phi_{xx} - guv - \phi + \phi^3 = 0, \quad u_x + g\phi u = \epsilon v, \quad -v_x + g\phi v = \epsilon u. \quad (6)$$

This system is supplemented by the normalization condition  $\int_{-\infty}^{\infty} dx (u^2 + v^2) = 1$ .

Consideration of the fermionic modes is usually related to the simplifying assumption that the scalar field background is fixed [13, 14]. In the decoupled limit  $g = 0$ , the  $\phi^4$  model supports a spatially localized static topological soliton, the kink, located at  $x = x_0$  and interpolating between the vacua  $\phi_0 = -1$  and  $\phi_0 = 1$ :

$$\phi_K(x) = \tanh(x - x_0). \quad (7)$$

For the sake of simplicity, we take  $x_0 = 0$ . The kink satisfies the Bogomolny equation  $d_x \phi_K = W'$ . The components of the spinor field on that external static background are solutions of the Schrödinger-type equations

$$(-\partial_x^2 + U_+(x)) u = \epsilon^2 u, \quad (-\partial_x^2 + U_-(x)) v = \epsilon^2 v \quad (8)$$

where  $U_\pm(x) = g^2 - g(g \pm 1) \text{sech}^2 x$  is the usual Pöschl-Teller potential. Thus, the zero mode  $\epsilon = 0$  is a particular solution of the Dirac equation [13, 14]:

$$\psi_0 \sim \begin{pmatrix} \text{sech}^g x \\ 0 \end{pmatrix}. \quad (9)$$

In the special case of the unbroken  $N = 1$  supersymmetry this mode is generated via the above-mentioned supersymmetry transformation of the field of the kink, and the configuration preserves half of the SUSY generators.

As the Yukawa coupling  $g$  increases, the potential well becomes deeper and new levels appear in the spectrum of the bound states, see the left plot of Fig. 1. We note that the energy spectrum of the localized fermions is symmetric with respect to inversion  $\epsilon \rightarrow -\epsilon$ , apart nodeless zero mode, which we will denote as  $A_0$ , each state with a positive eigenvalue  $\epsilon$  has a counterpart with reflected anti-symmetric  $u(v)$ -component and a negative eigenvalue  $-\epsilon$ , see Fig. 1, left plot. We classify the corresponding solutions according to their parity, there are two types of the boundary conditions for the massless fermions localized on the kink  $u_x|_0 = 0 \quad v|_0 = 0$  or  $u|_{x0} = 0 \quad v_x|_0 = 0$ . We refer to the modes of the first type to

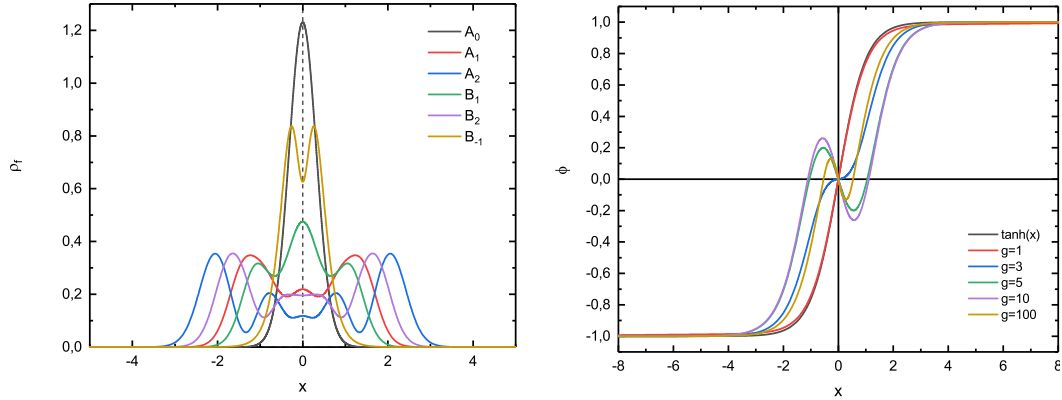


Figure 2: Left panel: The fermion density distribution of the fermion modes of different types localized on the kink in the absence of backreaction are plotted as functions of the coordinate  $x$  for  $g = 5$ . Right panel: The profiles of the field of the kink coupled to the backreacting fermionic mode  $B_1$  are plotted for several values of the Yukawa coupling  $g$ . Reprinted (without modification) from Ref. [25], ©2019 The Authors of [25] under the CC BY 4.0 license.

as  $A_k$ -modes and to the modes of the second tape to as  $B_k$ -modes. Here the index  $k$  corresponds to the minimal number of nodes of the components.

However, as the Yukawa coupling becomes stronger, the backreaction of the localized fermions could significantly affect the kink [25]. Indeed, for  $g \gtrsim 1$ , the self-consistent numerical solution of the coupled system of equations (5) becomes very different from the spectrum of fermions in the external field of the kink  $\phi_K$ , as displayed in the right plot of Fig. 2. The backreaction of the fermions breaks the symmetry between the localized modes with positive and negative eigenvalues. Localization of the fermions gives rise to spatial oscillations of the profile of the kink, where fermion modes are located. This configuration can be thought of as a chain of kink-antikink pairs tightly bounded by the localized fermions, and the number of the constituents on the chain increases for higher fermionic modes. Indeed,  $K\bar{K}$  pair can be stabilized by a collective fermionic mode localized between the solitons [26].

### 3 Fermion localization on the self-gravitating monopole

#### 3.1 Fermionic zero mode of the non-Abelian monopole

As a second example of fermionic mode localized on a soliton, we consider the (3+1)-dimensional  $SU(2)$  Yang-Mills-Higgs system coupled to the Dirac fermions in the flat space [14]:

$$L = \frac{1}{2} \text{Tr}(F_{\mu\nu} F^{\mu\nu}) + \text{Tr}(D_\mu \phi D^\mu \phi) - V(\phi) + L_{\text{sp}}, \quad (10)$$

where the covariant derivative of the scalar field in adjoint representation  $\phi = \phi^a \tau^a$  is  $D_\mu \phi = \partial_\mu \phi + ie[A_\mu, \phi]$  and  $e$  is the gauge coupling constant. The usual symmetry breaking potential is  $V(\phi) = \frac{\lambda}{4} \text{Tr}(\phi^2 - \phi_0^2)^2$ .

The bosonic sector of the model (10) is coupled to the Dirac isospinor fermions  $\psi$  with the Lagrangian [14] of the form

$$L_{\text{sp}} = \frac{i}{2} \left( (\hat{D}\bar{\psi})\psi - \bar{\psi}\hat{D}\psi \right) - \frac{i}{2} h \bar{\psi} \gamma^5 \phi \psi + m \bar{\psi} \psi, \quad (11)$$

where  $m$  is the bare fermion mass,  $h$  is the Yukawa coupling constant,  $\hat{D}_\mu \psi = (\partial_\mu + ieA_\mu)\psi$  and  $\gamma^\mu$  are the Dirac matrices in the standard representation.

The 't Hooft-Polakov monopole solution of the corresponding system of field equations

$$\begin{aligned} D_\nu F^{\nu\mu} &= -e\epsilon^{abc} \phi^b D^\mu \phi^c - \frac{e}{2} \bar{\psi} \gamma^\mu \sigma^a \psi, \\ D_\mu D^\mu \phi^a + \lambda \phi^a (\phi^2 - \phi_0^2) + ih \bar{\psi} \gamma^5 \sigma^a \psi &= 0, \\ i\hat{D}\psi - i\frac{h}{2} \gamma^5 \sigma^a \phi^a \psi - m\psi &= 0 \end{aligned}$$

is a topological map  $\Phi : S_\infty^2 \mapsto S_{vac}^2$ ,  $\Pi_2(S^2) = \mathbb{Z}$ , it can be constructed using the renowned static spherically symmetric hedgehog ansatz [8, 9]

$$\phi^a = \frac{r^a}{gr^2} H(r), \quad A_n^a = \varepsilon_{amn} \frac{r^m}{gr^2} [1 - W(r)], \quad A_0^a = 0. \quad (12)$$

For the spherically symmetric Dirac spin-isospinor fermions, we make use of the ansatz  $\psi = e^{-i\omega t} \begin{pmatrix} \chi \\ \eta \end{pmatrix}$ , where

$$\chi = \frac{u(r)}{\sqrt{2}} \begin{pmatrix} 0 & -1 \\ 1 & 0 \end{pmatrix}, \quad \eta = i \frac{v(r)}{\sqrt{2}} \begin{pmatrix} \sin \theta e^{-i\varphi} & -\cos \theta \\ -\cos \theta & -\sin \theta e^{i\varphi} \end{pmatrix} \quad (13)$$

and the normalization condition  $\int d^3x \psi^\dagger \psi = 1$  is imposed.

The dimensionless parameters of the model (10) are defined as the mass ratios  $\lambda = \frac{M_s}{M_v}$  and  $h = \frac{2M_f}{M_v}$ , where  $M_s$ ,  $M_v$ , and  $M_f$  are the masses of linearized excitations of the scalar, gauge and Dirac fields, respectively.

The system of non-linear coupled differential equations for four functions  $H, W, u$ , and  $v$  can be solved numerically, see, e.g., Ref. [44]; in general, it does not have an analytical solution. The only known exception is the self-dual Bogomolny-Prasad-Sommerfield (BPS) monopole, which exists in the limit of vanishing Higgs potential with non-zero vacuum expectation value of the scalar field  $\phi_0 = a$  [45, 46]:

$$W = \frac{x}{\sinh x}, \quad H = \coth x - \frac{1}{x}, \quad x = aer. \quad (14)$$

The corresponding equations for the spherically symmetric fermionic zero mode, localized on the BPS monopole, are

$$u' + u \left( \frac{1-W}{x} - \frac{h}{2} H \right) = 0, \quad v' + v \left( \frac{1+W}{x} + \frac{h}{2} H \right) = 0.$$

Integrating these equations, we easily obtain the normalizable solution for the localized zero mode,  $v = 0$ ,  $u \sim e^{-\int dx \left[ \frac{1-W(x)}{x} - \frac{h}{2} H(x) \right]}$ . It exists only for nonzero values of the scaled Yukawa coupling. Setting, for example,  $h = 2$  and making use of the exact BPS monopole solution (14), we obtain

$$v = 0, \quad u = \frac{1}{\cosh^2(x/2)}. \quad (15)$$

Notably, zero mode is unique, in the  $N = 1$  supersymmetric counterpart of the model (10) it arises as a result of SUSY variations of the field of the BPS monopole in the bosonic sector. Similar to the above-considered case of the  $N = 1$  supersymmetric kink, the monopole breaks down half of the supersymmetry; this configuration is referred to as the 1/2-BPS monopole. Variation of the Yukawa coupling  $h$  breaks the supersymmetry. However, since the eigenvalue of the Dirac operator for this mode remains zero for all values of  $h$ , it does not backreact on the bosonic sector. Situation becomes different for radial excitations of this mode, or in the case of non-zero bare mass term for the Dirac field. Another interesting scenario is observed when gravity is coupled to the monopole with localized fermion modes.

### 3.2 Fermion zero mode localized on a self-gravitating non-Abelian monopole

Let us now consider a self-gravitating non-Abelian monopole-fermion system [47]. The action of the model is:

$$S = \int d^4x \sqrt{-g} \left[ -\frac{R}{16\pi G} - \frac{1}{2} \text{Tr}(F_{\mu\nu} F^{\mu\nu}) + \text{Tr}(D_\mu \phi D^\mu \phi) - \frac{\lambda}{4} \text{Tr}(\phi^2 - \phi_0^2)^2 + L_{\text{sp}} \right], \quad (16)$$

where  $R$  is the scalar curvature,  $G$  is Newton's gravitational constant,  $g$  denotes the determinant of the metric tensor and the Dirac Lagrangian  $L_{\text{sp}}$  is defined by the eq. (11) above with the isospinor covariant derivative on a curved spacetime  $\hat{D}_\mu \psi = (\partial_\mu - \Gamma_\mu + ieA_\mu) \psi$ . Here  $\Gamma_\mu$  are the spin connection matrices.

Variation of the action (16) with respect to the metric leads to the Einstein equations

$$R_{\mu\nu} - \frac{1}{2} g_{\mu\nu} R = 8\pi G \left[ (T_{\mu\nu})_{YM} + (T_{\mu\nu})_\phi + (T_{\mu\nu})_s \right] \quad (17)$$

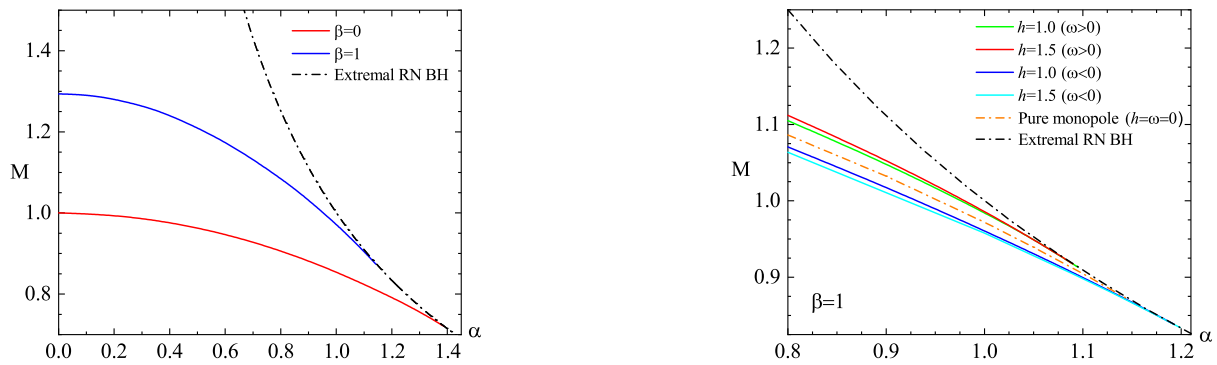


Figure 3: Left panel: The dependence of the ADM mass  $M$  of the gravitating monopole on the effective gravitational coupling  $\alpha$  is shown for  $\beta = 0$  and  $\beta = 1$  at  $h = -1$  and  $\omega = 0$ . Right panel: The same dependence is shown for the bounded monopole-fermion system with nonzero eigenvalues  $\omega$  for  $\beta = 1$  and  $h = 1, 1.5$ . For comparison, in both panels, the mass of the extremal Reissner-Nordström black hole of unit charge is also shown. Reprinted (without modification) from Ref. [47], ©2019 The Authors of [47] under the CC BY 4.0 license.

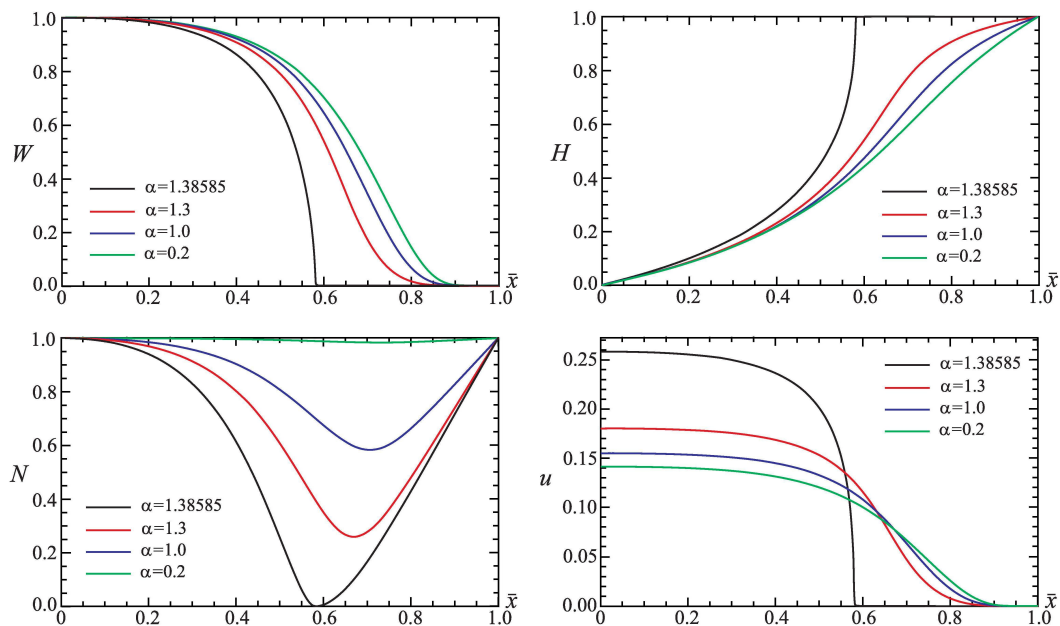


Figure 4: The profile functions of the solutions of the system (17) and (18) in the BPS limit  $\beta = 0$  are shown as functions of the compactified radial coordinate  $\bar{x} = x/(1+x)$  for some set of values of the effective gravitational coupling  $\alpha$  at  $\omega = 0$  and  $h = -1$ . The spinor component  $v$  always remains zero. Reprinted (without modification) from Ref. [47], ©2019 The Authors of [47] under the CC BY 4.0 license.

where  $(T_{\mu\nu})_{YM}, (T_{\mu\nu})_{\phi}$  and  $(T_{\mu\nu})_s$  are the corresponding components of the total stress-energy tensor.

The complete system of the field equations includes the matter field equations:

$$\begin{aligned} D_\nu F^{\alpha\nu\mu} &= -e\epsilon^{abc}\phi^b D^\mu\phi^c - \frac{e}{2}\bar{\psi}\gamma^\mu\sigma^a\psi, \\ D_\mu D^\mu\phi^a + \lambda\phi^a(\phi^2 - \phi_0^2) + ih\bar{\psi}\gamma^5\sigma^a\psi &= 0, \\ i\hat{D}\psi - i\frac{h}{2}\gamma^5\sigma^a\phi^a\psi &= 0. \end{aligned} \quad (18)$$

Considering spherically symmetric configurations, we implement the ansatz (12) and (13) and make use of the Schwarzschild-like line element

$$ds^2 = \sigma(r)^2 N(r) dt^2 - \frac{dr^2}{N(r)} - r^2(d\theta^2 + \sin^2\theta d\varphi^2) \quad (19)$$

parametrized by two functions  $N(r)$  and  $\sigma(r)$ . It is convenient to write the metric function  $N(r)$  as  $N(r) = 1 - \frac{2G\mu(r)}{r}$ ; then the ADM mass of the configuration is defined as  $M = \mu(\infty)$ .

The vierbein, which corresponds to the metric (19), is  $e^a_\mu = \text{diag}\left\{\sigma\sqrt{N}, \frac{1}{\sqrt{N}}, r, r\sin\theta\right\}$ , such that  $ds^2 = \eta_{ab}(e^a_\mu dx^\mu)(e^b_\nu dx^\nu)$  and  $\gamma^\mu = e^\mu_a \hat{\gamma}^a$  with  $\hat{\gamma}^a$  being the usual flat space Dirac matrices. Note that the system (17) and (18) admits embedded Reissner-Nordström (RN) solution with unit magnetic charge:

$$\sigma = 1, \quad \mu(x) = \mu_\infty - \frac{\alpha^2}{2x}, \quad W = 0, \quad H = 1, u = v = 0, \quad (20)$$

where  $\alpha^2 = 4\pi G\phi_0^2$ . A horizon occurs when  $N(x) \rightarrow 0$ ; in the Schwarzschild-like parametrization it happens at some finite critical value of  $x = x_{\text{cr}} = \alpha_{\text{cr}}$ .

The limit  $h \rightarrow 0$ , while  $\beta^2 = \frac{\lambda}{e^2}$  is kept fixed, corresponds to the decoupled fermionic sector. In such a case the well known pattern of evolution of the self-gravitating monopole is recovered, a branch of gravitating solutions emerges smoothly from the flat space monopole as the effective gravitational coupling  $\alpha$  increases from zero and  $\beta$  remains fixed [48, 49]. Along this branch the metric function  $N(x)$  develops a minimum, which decreases monotonically. The branch terminated at a critical value  $\alpha_{\text{cr}}$  at which the gravitating monopole develops a degenerate horizon and configuration collapses into the extremal RN black hole, as displayed in the left panel of Fig. 3.

The fundamental branch of gravitating BPS monopoles with bounded fermionic zero mode smoothly arises from the flat space configuration (14) and (15) as the effective gravitational constant  $\alpha$  is increased above zero. This branch reaches a limiting solution at maximal value  $\alpha_{\text{max}} = 1.403$ , where it bifurcates with the short backward branch which leads to the extremal RN black hole with unit magnetic charge, see Fig. 3.

Fig.4 displays solutions of the system system (17) and (18) for some set of values of the effective gravitational coupling  $\alpha$  at  $h = -1$  and  $\beta = 0$ . With increasing  $\alpha$  the size of the configuration with localized modes is gradually decreasing. As the critical value of  $\alpha$  is approached, the minimum of the metric function  $N(x)$  tends to zero at  $x = x_{\text{cr}}$ . The metric becomes splitted into the inner part,  $x < x_{\text{cr}}$  and the outer part,  $x > x_{\text{cr}}$ , separated by the forming horizon. The Higgs field takes the vacuum expectation value in exterior of the black hole, while the gauge field profile function  $W(x)$  trivializes there. As a result, the limiting configuration corresponds to the embedded extremal RN solution (20) with a Coulomb asymptotic for the magnetic field. At the same time, the fermion field becomes absorbed into the interior of the black hole, see Fig. 4.

Apart from the zero mode, the system of equations (17) and (18) supports a tower of regular normalizable fermionic modes with  $\omega \neq 0$ ,  $|\omega| < |h/2|$ . Here, both components  $u$  and  $v$  are non-zero, and for  $h < 0$  they possess at least one node while for  $h > 0$  they are nodeless. In the flat space limit these modes become delocalized as  $|\omega| \rightarrow |h/2|$ , while increasing of the gravitational coupling stabilizes the system. The general scenario is that, depending on the value of the Yukawa coupling constant  $h$ , there exists a critical value of the gravitational coupling  $\alpha_{\text{cr}}$  at which the spectral flow approaches the limit  $\omega \rightarrow \pm 0$  and the configuration runs into the embedded RN solution (20).

#### 4 Fermion zero mode localized on a self-gravitating Skyrmion

Finally, we consider the (3+1)-dimensional Einstein-Skyrme system coupled to a spin-isospin Dirac field [43]:

$$S = \int d^4x \sqrt{-g} \left( -\frac{R}{16\pi G} + \mathcal{L}_m \right), \quad (21)$$

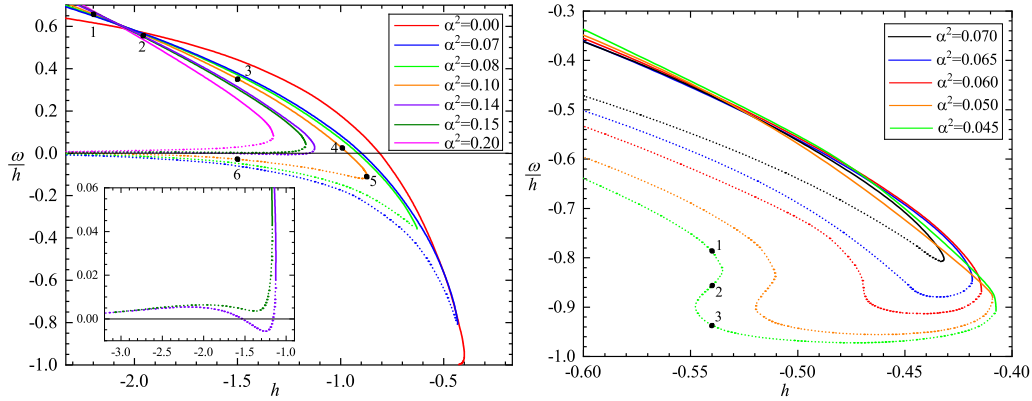


Figure 5: The scaled eigenvalue  $\omega/h$  of the localized fermionic mode is shown versus the Yukawa coupling  $h$  for several values of the effective coupling  $\alpha^2$ . The inset in the left plot highlights the presence of multiple branches close to the transition of the bifurcation point from positive to negative eigenvalues of  $\omega$ . Right plot illustrates the multibranch structure for small values of  $\alpha$ .

where, by analogy with (16), the gravitational part is the Einstein-Hilbert action, and  $\mathcal{L}_m = \mathcal{L}_{\text{Sk}} + \mathcal{L}_{\text{sp}} + \mathcal{L}_{\text{int}}$ . Here the Skyrme Lagrangian is [7]

$$\mathcal{L}_{\text{Sk}} = -\frac{f_\pi^2}{4} \text{Tr} (\partial_\mu U \partial^\mu U^\dagger) + \frac{1}{32a_0^2} \text{Tr} \left( [\partial_\mu U U^\dagger, \partial_\nu U U^\dagger]^2 \right), \quad (22)$$

and  $f_\pi$  and  $a_0$  are the parameters of the model with dimensions  $[f_\pi] = L^{-1}$  and  $[a_0] = L^0$ , respectively. It is convenient to introduce the dimensionless radial coordinate  $r \rightarrow a_0 f_\pi r$ , the effective gravitational coupling  $\alpha^2 = 4\pi G f_\pi^2$ , and to rescale the Dirac field, the Yukawa coupling constant and the bare fermion mass as  $\psi \rightarrow \psi / \sqrt{a_0 f_\pi^3}$ ,  $h \rightarrow h / (a_0 f_\pi)$ , and  $m \rightarrow m / (a_0 f_\pi)$ , respectively.

The Dirac Lagrangian is again given by eq. (11) with the isospinor covariant derivative on a curved spacetime and the Skyrme-fermion chiral interaction Lagrangian is  $\mathcal{L}_{\text{int}} = h \bar{\psi} U \gamma^5 \psi$ ,  $U \gamma^5 \equiv \frac{\mathbb{1} + \gamma_5}{2} U + \frac{\mathbb{1} - \gamma_5}{2} U^\dagger$ .

Contrary to the case of the spectrum of the Dirac fermions localized on the monopole in Minkowski spacetime, the eigenvalue of the Dirac operator always depends on the strength of the Yukawa coupling. However, in agreement with the index theorem, the normalizable bound mode crossing zero is unique. Note that, in general, there is no self-dual truncation of the Skyrme model, also its supersymmetric extension is related with non-linear realization of supersymmetry, see e.g. [50].

The matrix-valued Skyrme field  $U \in SU(2)$  can be decomposed into the scalar component  $\phi_0$  and the pion isotriplet  $\phi_n$  via  $U = \phi_0 \mathbb{1} + i\phi_n \tau_n$ , where  $\tau_n$  are the Pauli matrices, and the field components  $\phi^a = (\phi_0, \phi_n)$  are subject to the sigma-model constraint,  $\phi^a \cdot \phi^a = 1$ .

To construct spherically symmetric solutions of the model (21), we employ Schwarzschild-like coordinates (19) and make use of the conventional hedgehog parametrization  $U = \cos(F(r)) \mathbb{1} + i \sin(F(r)) (\sigma^a n^a)$ , where  $n^a$  is the unit radial vector. The Skyrme profile function  $F(r)$  corresponds to the configuration of topological degree one. Again, for the isospinor fermion field localized on the Skyrme, we implement the spherically symmetric ansatz (13) with two real functions of the radial coordinate only.

In the decoupled limit ( $h \rightarrow 0$ ) the dependence of the regular self-gravitating Skyrme on the effective gravitational coupling  $\alpha^2 = 4\pi G f_\pi^2$  is well known. There are two branches of solutions which are characterized by their limiting behavior as  $\alpha$  tends to zero [51]. The first branch originates from the flat spacetime Skyrme, it extends up to a maximal value  $\alpha_{\text{max}}^2 \approx 0.0404$ , where it bifurcates with the second, upper mass branch. The second (backward) branch extends down to the limit  $\alpha \rightarrow 0$  which is approached as  $f_\pi \rightarrow 0$ . Thus the sigma-model term in the Skyrme Lagrangian (22) is vanishing and the configuration tends to the scaled Bartnik-McKinnon (BM) solution. We will refer to them as the Skyrme branch and the BM branch, respectively.

In the presence of the fermions, the limit  $\alpha = 0$  with  $G = 0$  corresponds to the fermionic mode localized on the Skyrme in Minkowski spacetime. Unlike the monopole counterpart, which always has zero eigenvalue of the Dirac operator, this mode emerges from the positive continuum at some critical value of the Yukawa coupling  $h_{\text{cr}} \approx -0.40$ . Further increase of the modulus of the Yukawa coupling



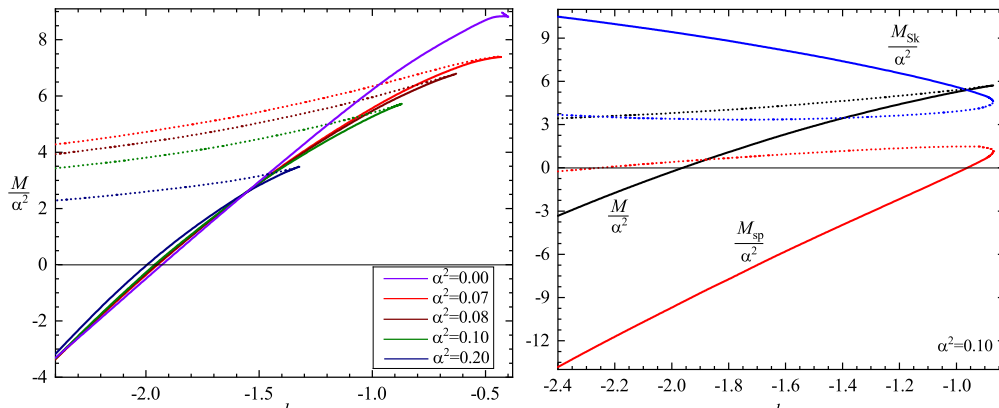


Figure 6: Left panel: The scaled ADM mass  $M/\alpha^2$  of the gravitating Skyrmion-fermion system is shown versus the Yukawa coupling  $h$  for a set of values of the effective coupling  $\alpha^2$ . Right panel: The contributions to the scaled total ADM mass ( $M/\alpha^2$ , black) from the fermion ( $M_{\text{sp}}/\alpha^2$ , red) and the Skyrme ( $M_{\text{Sk}}/\alpha^2$ , blue) fields are shown versus the Yukawa coupling  $h$  for effective coupling  $\alpha^2 = 0.1$ .

decreases the scaled eigenvalue  $\omega/|h|$  of the Dirac operator. For some critical value of the coupling  $h$  the curve  $\omega(h)$  then crosses zero, as seen in Fig. 5. There is a single fermionic level which monotonically flows from positive to negative values as the coupling decreases.

More generally, there is a family of solutions depending continuously on two parameters, the Yukawa coupling constant  $h$  and the eigenvalue of the Dirac operator  $\omega$ , for each particular value of the effective gravitational coupling  $\alpha$ . Since the appearance of a single zero crossing fermionic level is related to the underlying topology of the Skyrme field, we may expect that, as the self-gravitating configuration evolves towards the topologically trivial BM solution, this mode undergoes a certain transition.

Indeed, for any non-zero value of the gravitational coupling, the spherically symmetric fermionic mode localized on the Skyrme is no longer linked to the positive continuum, as seen in Fig. 5. Instead, it arises at some particular value of the Yukawa coupling  $h_{\text{max}}(\alpha) < h_{\text{cr}}$  with a scaled eigenvalue  $\omega/|h|$  smaller than the threshold value. Physically, this situation reflects the energy balance of the system of a self-gravitating Skyrme dressed by the fermions: the added gravitational interaction must be compensated by the force of the Yukawa interaction.

The multiple branch structure can be associated with the form of the dimensionless Yukawa coupling  $h \rightarrow h/(a_0 f_\pi)$  when the same value of the coupling  $h$  may correspond to different choices of all three parameters. Further, variation of the parameter  $f_\pi$  may be related to a corresponding change of the effective gravitational constant  $\alpha$ .

An intriguing pattern is observed in the dependency of the scaled ADM mass  $M/\alpha^2$  on the Yukawa coupling  $h$ , see Fig. 6. For a given value of the Yukawa coupling  $h$ , the mass of the configurations on the Skyrme branch is smaller than the mass on the BM branch. With increasing  $\alpha$  the mass of the configurations on the BM branches, including the bifurcation points, decreases. In contrast, the mass on the lower parts of the Skyrme branches does not vary significantly as  $\alpha$  is increased.

Interestingly, the ADM mass on the Skyrme branches crosses zero when the Yukawa coupling is decreased, as demonstrated in Fig. 6. Inspection of the configurations at this critical point with  $M = 0$  shows that the metric component  $g_{00}$  is nearly unity almost everywhere in space, and that the first derivative of the metric function  $N$  at spatial infinity vanishes. Beyond this critical point, the ADM mass of the backreacting Skyrme-fermion system becomes *negative* as the Yukawa coupling  $h$  decreases along the Skyrme branch, as seen in Fig. 6. While surprising at first, this hints at the capacity of fermions to violate the energy conditions [43].

## Acknowledgments

Y.S. is very grateful to the organizers of the XXVIII International Conference on Integrable Systems and Quantum Symmetries, where this work was presented. He also thank Ilya Perapechka for valuable collaboration, many results of our joint work are reviewed in this brief survey. Y.S. gratefully acknowledges the support of the Alexander von Humboldt Foundation and HWK Delmenhorst. This research was supported by the Ministry of Science and Higher Education of the Republic of Kazakhstan (Grant No. AP23490322 ‘‘Exploration of Thermodynamic Properties of Relativistic Compact Objects within the

Framework of Geometrothermodynamics (GTD)”).

## References

- [1] Manton N and Sutcliffe P 2004 *Topological solitons* (Cambridge University Press)
- [2] Shnir Y 2018 *Topological and Non-Topological Solitons in Scalar Field Theories* (Cambridge University Press)
- [3] Nielsen H and Olesen P 1973 *Nucl. Phys.* **B 61** 45
- [4] Polyakov A and Belavin A 1975 *JETP Lett.* **22** 245
- [5] Bogolubskaya A and Bogolubsky I 1989 *Phys. Lett. A* **136** 485 (1989)
- [6] Piette B *et al* 1994 *Phys. Lett. B* **320** 294
- [7] Skyrme T 1961 *Proc. Roy. Soc. Lond.* **A 260** 127
- [8] 't Hooft G 1974 *Nucl. Phys. B* **79** 276
- [9] Polyakov A 1974 *JETP Lett.* **20** 194
- [10] Atiyah M, Patodi V, and Singer I 1975 *Math. Proc. Cambridge Phil. Soc.* **77** 43
- [11] Caroli C, De Gennes P, and Matricon J 1964 *Phys. Lett.* **9(4)** 307
- [12] Jackiw R and Rossi P 1981 *Nucl. Phys. B* **190** 681
- [13] Dashen R, Hasslacher B, and Neveu A 1974 *Phys. Rev. D* **10** 4130
- [14] Jackiw R and Rebbi C 1976 *Phys. Rev. D* **13** 3398
- [15] Rubakov V 1982 *Nucl. Phys. B* **203** 311
- [16] Callan C Jr. 1982 *Phys. Rev. D* **26** 2058
- [17] Witten E 1985 *Nucl. Phys. B* **249** 557
- [18] Di Vecchia P and Ferrara S 1977 *Nucl. Phys. B* **130** 93
- [19] Novikov V *et al* 1984 *Phys. Rept.* **116** 103
- [20] Adam C *et al* 2011 *Phys. Rev. D* **84** 025008
- [21] Kahana S, Ripka G and Soni V 1984 *Nucl. Phys. A* **415** 351
- [22] Ripka G and Kahana S 1985 *Phys. Lett.* **155B** 327
- [23] Perapechka I, Sawado N and Shnir Ya 2018 *JHEP* **1810** 081
- [24] Perapechka I and Shnir Ya 2019 *Phys. Rev. D* **99** 125001
- [25] Klimashonok V, Perapechka I and Shnir Ya 2019 *Phys. Rev. D* **100** 105003
- [26] Perapechka I and Shnir Ya 2020 *Phys. Rev. D* **101** 021701
- [27] Campos J *et al* 2023 *JHEP* **01** 071
- [28] Weigel H and Saadatmand D 2024 *Universe* **10** 13
- [29] Bazeia D, Campos J and Mohammadi A 2022 *JHEP* **12** 085
- [30] Gani V *et al* 2022 *Eur. Phys. J. C* **82** 757
- [31] Amari Y, Sawado N and Yamamoto S 2024 *JHEP* **06** 057
- [32] Taub A 1937 *Phys. Rev.* **51** 512
- [33] Finster F, Smoller J and Yau S. T. 1999 *Phys. Rev. D* **59** 104020
- [34] Herdeiro C *et al* 2019 *Phys. Lett. B* **797** 134845
- [35] Dzhunushaliev V and Folomeev V 2019 *Phys. Rev. D* **99** 084030
- [36] Dzhunushaliev V and Folomeev V 2019 *Phys. Rev. D* **99** 104066
- [37] Blázquez-Salcedo J and Knoll C 2020 *Eur. Phys. J. C* **80** 174
- [38] Herdeiro C *et al* 2022 *Phys. Lett. B* **824** 136811
- [39] Blázquez-Salcedo J, Knoll C and Radu E 2021 *Phys. Rev. Lett.* **126** 101102
- [40] Bolokhov S *et al* 2021 *Grav. Cosmol.* **27** 401
- [41] Armendariz-Picon C and Greene P. B. 2003 *Gen. Rel. Grav.* **35** 1637
- [42] Cai Y. F. and Wang J 2008 *Class. Quant. Grav.* **25** 165014
- [43] Dzhunushaliev V *et al* 2024 *Phys. Lett. B* **855** 138812
- [44] 2005 Shnir Ya M *Magnetic Monopoles* (Springer)
- [45] Bogomolny E 1976 *Sov. J. Nucl. Phys.* **24** 449
- [46] Prasad M and Sommerfield C 1975 *Phys. Rev. Lett.* **35** 760
- [47] Dzhunushaliev V, Folomeev V and Shnir Ya 2023 *Phys. Rev. D* **108** 065005
- [48] Lee K, Nair V and Weinberg E 1992 *Phys. Rev. D* **45** 2751
- [49] Breitenlohner P, Forgacs P and Maison D 1992 *Nucl. Phys. B* **383** 357
- [50] Gudnason S B, Nitta M and Sasaki S 2016 *JHEP* **02** 074
- [51] Bizon P and Chmaj T 1992 *Phys. Lett. B* **297** 55